33rd Annual International Conference of the IEEE EMBS
Boston, Massachusetts USA, August 30 - September 3, 2011

Vibro-acoustography and B-mode integration for 3D imaging

Hermes A. S. Kamimura, Marden A. Fagundes, Mostafa Fatemi, *Senior Member, IEEE*
and Antonio A. O. Carneiro

***Abstract*— Tridimensional representation of vibro-acoustography images based on the topology acquired by B-mode acquisitions is proposed for the evaluation of bone and implant surfaces. A tridimensional evaluation of the implant coverage used in a total hip arthroplasty procedure was performed to show the feasibility of this approach. A vibro-acoustography image of the uncovered area of the implant was acquired and represented in planar representation. However, tridimensional representation of the exposed surface area is necessary for proper evaluation of the stability of the implant. Hence, the topologies of the implant and the bone region around it were determined by acquiring 280 B-mode images. The B-scan images were processed in order to reconstruct the tridimensional surface of the objects. Finally, the vibro-acoustography image and the B-mode-based surface were aligned for the tridimensional visualization. The B-mode tridimensional representation of the bone and implant was improved by the enhancement of contrast and resolution provided by the vibro-acoustography image. The final tridimensional image presented a resolution of 0.25 mm. The topological correction based on B-mode slices allowed an accurate evaluation of the surface area.**

I. INTRODUCTION

Current X-ray-based methods are not feasible for postoperative monitoring in some cases of therapeutic procedures due to the impossibility of wide visualization of the region, side effects in patients or image artifacts. Total hip arthroplasty (THA) is a cost-effective procedure to treat patients with end stage osteoarthritis in which implants replace the head of the femur and the acetabular in the pelvis [1]. Plain AP (anterior/posterior) pelvis radiographs are used in this case for measuring the cup coverage postoperatively [2] [3]. However, to provide precise information relating the minimum cup coverage and cup loosening rate, a noninvasive three-dimensional imaging technique is required, since plain AP radiograph does not allow clear visualization of the both anterior and posterior regions [4] (Fig. 1). Since, X-ray radiograph is avoided in cases involving children [5], B-mode ultrasound images allow an estimation of the investigated regions. Other modalities such as computer tomography and magnetic resonance imaging introduce artifacts due to the material used in the implants (metal and ceramic), which can be a problem for a correct evaluation of the uncovered area.

Ultrasound wave (UW) propagation is subjected to energy loss by absorption, where its energy is converted into other energy forms such as heat, chemical energy, or light [6]. Changes in the compressibility and density of the medium can cause scattering (mainly reflection and refraction) of the wave. Objects inside the human body with high densities, such as bones and metal implants used in orthopedic procedures, present high impedance causing high reflection of the UW. For high-density objects, UW propagation is severely attenuated. Ultrasound parameters (frequency, intensity, contrast, etc) can be set to mainly display information about the surface of high-density objects. Therefore, high-density helps the visualization of the surface in ultrasound modalities in comparison to X-ray-based modalities where the high-density can include artifacts or blind regions anterior or posterior to the object.

Vibro-acoustography (VA) is an ultrasound-based technique in which two cofocused ultrasound beams of slightly different frequency (MHz) generate a low frequency (kHz) acoustic excitation due to their interference [7] [8]. A dedicated hydrophone detects the sound emitted by the target when excited by this low frequency radiation force. The focused low-frequency excitation provides a speckle-free image with a high lateral resolution image (sub-mm). Calle [9] presented VA images with high resolution of the trabecular structure of a calcaneus bone. An implementation of VA on a clinical imaging system [10] using linear and phased arrays is being developed in Mayo Clinic which

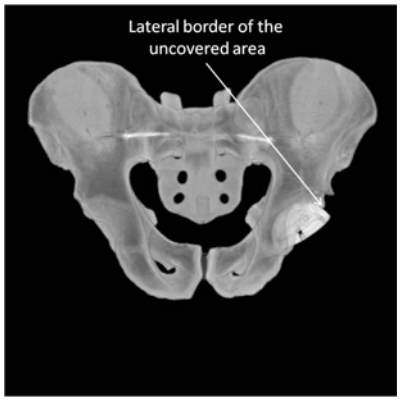

Fig. 1. Plain AP (anterior/posterior) radiography of the total hip arthroplasty model. The uncovered area is not clear in the anterior and posterior region. The implant coverage is evaluated by defining the lateral border of the uncovered region.

This work was supported by Conselho Nacional de Desenvolvimento Cientifico e Tecnologico (CNPq) from Brazil.

Hermes A. S. Kamimura Marden A. Fagundes, and Antonio Adilton O. Carneiro are with the Departamento de Fisica, Faculdade de Filosofia Ciencias e Letras de Ribeirao Preto, Universidade de Sao Paulo, Ribeirao Preto, SP, Brazil. (adilton@ffclrp.usp.br)

Mostafa Fatemi is with the Department of Physiology and Biomedical Engineering, Mayo Clinic, College of Medicine, Rochester, MN, 55904, USA

allows more clinically oriented studies with VA.

In this work, we propose the 3D correction of the topology of VA images based on tridimensional US [11]. This method is presented as an alternative for the postoperative evaluation of the uncovered area of implants used in THA. Other potential applications of the proposed imaging method are the evaluation of bones and implants in shallow tissues used in arms and legs in orthopedic treatments.

II. Materials and Methods

A. Total hip arthroplasty model

An acetabular implant cup with an outer diameter of 57.10 $\pm$ 0.05 mm (Amplitude, France) was inserted inside a foam bone model of typical adult pelvis size and elastic modulus of 210 MPa (Sawbones model 1301-1, USA) to simulate THA.

The region around the pelvis (muscle and fat layers) was simulated using a tissue-mimicking material composed of evaporated milk (0.9 L), porcine skin-derived gel (180 g), glycerol (180 mL), potassium sorbate (18 g), and water (0.9 L). We assumed empirical values for the attenuation coefficients of fat and skeletal muscles of $\alpha_f = 0.48$ dB.cm^{-1} and $\alpha_m = 0.74$ dB.cm^{-1} [12], respectively. The proportion of 2/3 of muscle/fat layers, would present a resultant attenuation coefficient of $\alpha_r = 0.58$ dB.cm^{-1}. The dilution of evaporated milk in water allowed us to control the attenuation coefficient [13]. The tissue phantom exhibited characteristics very similar to the actual soft tissue *in vivo* with attenuation of about 0.5 dB.cm^{-1}, propagation speed of 1500 m.s^{-1} and 5 cm thickness.

B. Area estimation

An independent measurement of the uncovered implant area was previously evaluated for further comparison with the proposed method. First, the Optotrak Certus^{TM}capture system (NDI, Canada) acquired points on the edge of the implant and on the border of its uncovered area. Then, using the Solidworks^{TM}CAD software (Dassault Systemes, France), a surface plane representing the region of interest was reconstructed based on the 3D curve passing through the acquired points. The accuracy of the method was 0.15 mm. Finally, the uncovered area was calculated by using the surface area evaluation tool of SolidWorks^{TM}.

C. Vibro-acoustography acquisition

The VA system was composed of a three-axis scanner system (0.25 mm resolution), two function generators (Tektronix model AFG320), a confocal transducer (45 mm of outer diameter and 7 cm of focal distance), a hydrophone (International Transducer Corp. model ITC-6080C), a filter (Stanford Research System model SR650), and a computer. The THA model was immersed inside a tank with degassed water (Fig. 2).

The confocal transducer swept the pelvic model in a 5 cm x 7 cm raster pattern. Three acquisition planes, at 5.3 cm, 5.8 cm and 6.3 cm depths, were acquired and combined in one image to enlarge the focus coverage on the implant exposed area. The uncovered implant area was identified by analyzing the image texture using contour segmentation [14].

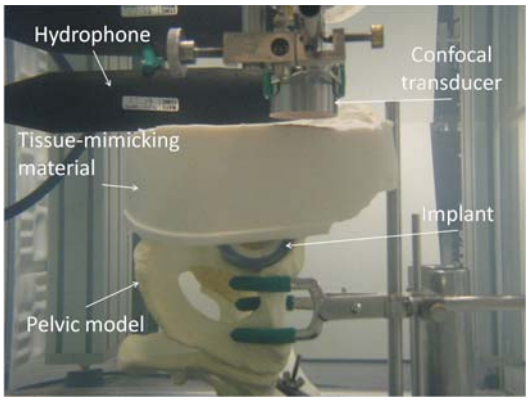

Fig. 2. Vibro-acoustography acquisition setup using a confocal ultrasound transducer and a tissue-mimicking gel to simulate the soft tissue around the hip.

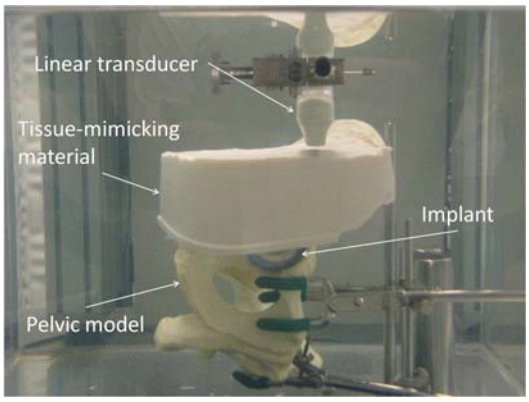

Fig. 3. B-scan acquisition setup using a linear transducer. This acquisition was performed in order to reconstruct the tridimensional surface of the implant and bone around it.

D. B-scan acquisition

B-mode image acquisitions of the THA model in 3D linear scanning mode [11] using a linear-array transducer with GE Vivid 7 machine were acquired to provide tridimensional topology correction (Fig. 3). 280 B-mode images with 0.25 mm of distance between each pair of slices were acquired providing a volume. The contrast of the image was set to avoid speckle noise and to reveal the surface profile of the bone and implant.

The 3D correction was performed by detecting the tridimensional profile of the THA model in the 280 slices. The detected profiles in each slice were joined to form the surface of the model based on feature-based reconstruction [15].

A threshold to keep only values greater than 80% of the maximum pixel value was applied in the B-mode slices. The remaining speckle was reduced by applying a median filter. Then, for each image, the profile was binarized by selecting the pixels with maximum value in each column. The profiles contained some gaps that were closed by interpolation. The final 3D surface was obtained by merging the profiles and

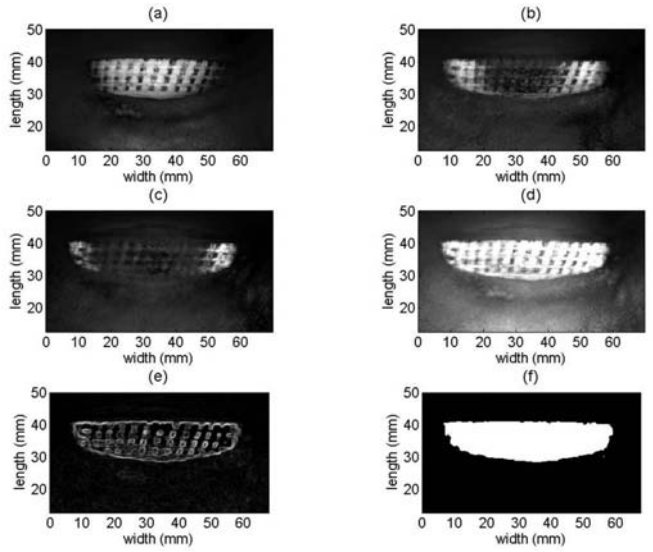

Fig. 4. Vibro-acoustography images. (a) VA image at 5.3 cm of depth, (b) VA image at 5.8 cm of depth, (c) VA image at 6.3 cm of depth, (d) linear combination with equal weighting of images, (e) texture (by contour) of the uncovered implant area, and (f) segmented region.

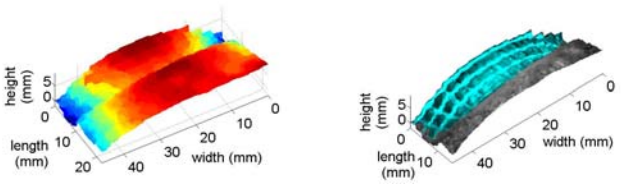

(a) (b)

Fig. 5. Tridimensional representation of the implant topology using the B-mode approach: (a) B-mode-based topology and (b) Tridimensional image result.

applying the segmented VA image as texture.

The total surface area of the implant is equal to $2.\pi.r^2$. Once the topology correction was applied, the segmented area in the VA image defined the surface area to be evaluated. The surface area was numerically computed by calculating the sum of the triangular sub-areas formed by three neighboring pixels. The sub-areas (of the triangles) were calculated by the cross product of the vectors defined by the vertices [16].

III. Results

The combination of the VA images (Fig. 4(d)) in three different depths (Fig. 4(b), (c), and (d)) enlarged the focal depth coverage on the exposed area of the implant. The segmentation process based on the contour (Fig. 4(e)) identified the region of interest (Fig. 4(f)) allowing evaluation of the area of the uncovered implant.

Fig. 5(a) shows the tridimensional surfaces of the implant and bone around it. The VA image was merged to the 3D representation of the model to allow visualization of the uncovered implant area (Fig. 5(b)).

The metal implant diameter was 5.71 cm and its total surface area was 51.2 cm^2. The estimated uncovered area provided by the optic measurements was 6.64 cm^2 and represented 13.0 % of the half sphere.

The VA image exhibited high contrast between metal and bone which revealed implant surface texture. The proposed method for tridimensional evaluation provided an area of 6.30 cm^2 or 12.3 % of $1/2$ of the sphere area (Fig. 5).

IV. Discussion

Previous works involving VA have proved the feasibility of the technique for soft tissue evaluation. This work presented tridimensional VA images of an implant and pelvic bone as an alternative postoperative evaluation of implant stability used in THA. The tridimensional surface correction was based on B-scan images, which allowed an accurate evaluation of the uncovered implant area.

Despite the inherent problems in the B-scan acquisition system, such as reverberation, shadowing, and scattering due to the incident angle, this modality with appropriate image processing provides information of object distance, which is neglected in VA mode. In our work, we showed that VA and B-scans can be used together in the enhancement of 3D surface representation of unknown shapes of bones or other object inside the tissue. These two techniques can be combined and potentially facilitate the surgical procedure and postoperative evaluation for the improvement of the longevity of prosthetic components.

The 3D images were generated and processed in *Matlab* ® R2008a which allows the interchangeability of part models between the Matlab and Solidworks. It can be useful for the design of new implants with better coupling with bones.

V. Conclusion

The tridimensional correction of the VA image provided a quantitative evaluation of the uncovered implant surface area. The use of B-scans and VA together allowed the visualization of the bone surface around the implant and a more accurate evaluation of the stability of the implant. It may also useful for detecting some cracks in the pelvis. Furthermore, for high density objects with unknown geometries, VA and B-mode ultrasound images can be used together for surface evaluation.

The implementation of this approach in clinic can be improved using the same transducer for both B-mode and VA modalities. By using the same transducer, images provided by both methods can be easily matched decreasing the time of image processing and avoiding problems caused by differences in the transducers positions. The implementation of VA on a clinical imaging system would facilate the integration of the methods.

VI. Acknowledgments

The authors would like to thank Dr. James F. Greenleaf and Dr. Kai-Nan An for their support in technical discussions.

REFERENCES

[1] T. E. Brown, Q. Cui, and W. M. Mihalko, *Arthritis and arthroplasty: The hip*, ser. Arthritis and Arthroplasty. Philadelphia: Saunders Elsevier, 2009. 428 p. [Online]. Available: http://books.google.com.br/books?id=Roy4xpcvQLsC

[2] M. J. Anderson and W. H. Harris, "Total hip arthroplasty with insertion of the acetabular component without cement in hips with total congenital dislocation or marked congenital dysplasia," *J. Bone Jt. Surg. (Am.)*, vol. 81A, no. 3, pp. 347–354, Mar. 1999.

[3] G. Hartofilakidis, G. Georgiades, G. C. Babis, and C. K. Yiannakopoulos, "Evaluation of two surgical techniques for acetabular reconstruction in total hip replacement for congenital hip disease - Results after a minimum ten-year follow-up," *J. Bone Jt. Surg. (British)*, vol. 90B, no. 6, pp. 724–730, Jun. 2008.

[4] M. J. Spangehl, D. J. Berry, R. T. Trousdale, and M. E. Cabanela, "Uncemented acetabular components with bulk femoral head autograft for acetabular reconstruction in developmental dysplasia of the hip: results at five to twelve years," *J. Bone Jt. Surg.*, vol. 83A, no. 10, pp. 1484–1489, out. 2001.

[5] D. Reynolds and M. A. R. Freeman, *Osteoarthritis in the young adult hip: options for surgical management*, ser. Current problems in orthopaedics. Churchill Livingstone, 1989. 290 p. [Online]. Available: http://books.google.com.br/books?id=Nl5sAAAAMAAJ

[6] R. S. C. Cobbold, *Foundations of biomedical ultrasound*. Oxford University Press, USA, 2007.

[7] M. Fatemi and J. F. Greenleaf, "Ultrasound-stimulated vibro-acoustic spectrography," *Science*, vol. 280, no. 5360, pp. 82–85, Apr. 1998.

[8] ——, "Vibro-acoustography: An imaging modality based on ultrasound-stimulated acoustic emission," *Proc. Nat. Acad. of Sci. USA*, vol. 96, no. 12, pp. 6603–6608, Jun. 1999.

[9] S. Calle, J. P. Remenieras, O. B. Matar, M. Defontaine, and F. Patat, "Application of nonlinear phenomena induced by focused ultrasound to bone imaging," *Ultrasound Med. Biol.*, vol. 29, no. 3, pp. 465–472, 2003.

[10] M. W. Urban, C. Chalek, R. R. Kinnick, T. M. Kinter, B. Haider, J. F. Greenleaf, K. Thomenius, and M. Fatemi, "Implementation of vibro-acoustography on a clinical ultrasound system," *IEEE Trans. Ultrason. Ferroelectr. Freq. Control*, In review.

[11] Nelson T. R. and Pretorius, D. H., "Three-dimensional ultrasound imaging," *Ultrasound Med. Biol.*, vol. 24, no. 9, pp. 1243 – 1270, 1998.

[12] T. D. Mast, "Empirical relationships between acoustic parameters in human soft tissues," *Acoustics Research Letters Online*, vol. 1, no. 2, pp. 37–42, 2000.

[13] E. L. Madsen, G. R. Frank, and F. Dong, "Liquid or solid ultrasonically tissue-mimicking materials with very low scatter," *Ultrasound Med. Biol.*, vol. 24, no. 4, pp. 535–542, May. 1998.

[14] Pal, N. R. and Pal, S. K. , "A review on image segmentation techniques," *Pattern Recognition*, vol. 26, no. 9, pp. 1277 – 1294, 1993.

[15] A. Fenster, D. B. Downey, and H. N. Cardinal, "Three-dimensional ultrasound imaging," *Physics Med. Biol.*, vol. 46, no. 5, pp. R67–R99, May. 2001.

[16] D. G. Zill and M. R. Cullen, *Advanced engineering mathematics*, 3rd ed. Jones and Bartlett Publishers, Inc., 2006, ch. 7.4 Cross Product, pp. 319–324.